JOURNAL OF SPACECRAFT AND ROCKETS
Vol. 31, No. 6, November–December 1994

Structural Design and Mitigation of Mirror Deformations in Lunar-Based Telescopes

Paul L. Luz*
NASA Marshall Space Flight Center, Huntsville, Alabama 35812

Structural design and analysis of the optical systems for lunar-based telescopes is a challenging task. A driving concern of the Lunar Ultraviolet Telescope Experiment (LUTE) preliminary design study was the degradation of the LUTE optical figure due to thermal deformations, during a temperature cycle of 65 to 265 K at the reference 40 deg latitude, 0 deg longitude landing site. In addressing this task, temperature effects were characterized, and primary-mirror thermal deformations calculated for use in the optical analyses. Trade studies evaluated the qualitative performance of various design schemes. Results indicated that statically determinate mirror supports with bottom-mounted flexures created less optical disturbance under thermal loading than mirror supports at the inner or outer periphery. Another trade indicated that a telescope's baseplate must be athermalized with respect to the mirrors by matching thermal distortion coefficients. A comparison of three materials for the primary mirror predicted that silicon carbide would be the best material for resisting thermally induced figure deformations on the moon.

Nomenclature

AR	= athermalization ratio
BTE	= bulk temperature excursion, $\int(\partial T/\partial t)\,dt$, K
C_p	= specific heat, J/kg-K
CTE	= coefficient of thermal expansion, ppm/K
E	= Young's modulus of elasticity, GPa
FEM	= finite-element model
k	= thermal conductivity, W/m-K
	= stiffness, N/m (structures)
	= extinction coefficient (optics)
L	= length, cm
LUTE	= Lunar Ultraviolet Telescope Experiment
n	= index of refraction
ppm	= parts per million
r	= radial location, cm
ρ	= mass density, kg/m^3
SiC	= silicon carbide
SSTDC	= steady-state thermal distortion coefficient, cm/MW.
t	= thickness, cm
T	= temperature, K
T_0	= reference temperature, K
TTDC	= transient thermal distortion coefficient, μs/cm^2-K
YTS	= yield tensile strength, MPa
λ	= wavelength, Å

Introduction

STRUCTURAL design of the optical systems for lunar-based telescopes poses a significant challenge to the analyst, due to the lunar thermal environment. Lunar-based telescope have to contend with thermally induced degradation of their optical figure and performance because of the large temperature swings associated with the lunar environment. This paper will present results from structural trade studies of the Lunar Ultraviolet Telescope Experiment (LUTE),[1] in hope that this information will prove useful for the design of lunar-based telescopes in general. The LUTE, pictured in Fig. 1, is a 1-m-class telescope to be landed on the lunar surface and remotely operated from Earth. It is designed to observe the ultraviolet spectrum, the wavelength of interest being 1000–3500 Å (Ref. 2). It has a 2-yr minimum life requirement and may serve as a precursor mission for returning to the moon.

The optical design for the LUTE, drawn in Fig. 2, is a compact 1-m-aperture, three-mirror system with a 1.4-deg field of view and a system focal length of 300 cm. The image diameter is 7.4 cm, and the separation distance between the primary, secondary, and tertiary mirrors is 65 cm.

Design Environment for Lunar Operation of the LUTE

The LUTE was designed to launch on an Atlas II/AS. Mass and power constraints for lunar delivery and operation of the LUTE were challenging. The baseline thermal control system, consequently, was designed to be passive, meaning no heaters. Likewise, the baseline optical control system was not designed with actuators to bend and deform the mirrors.

Operating in the lunar environment under these conditions imposed some substantial requirements on the optical structures. Thermal data shows that the lunar surface temperature can vary from 93 K at sunrise to as hot as 395 K at local noon.[3] During this 14-day lunar day night cycle, thermal analysis[4] predicted that the temperature of the LUTE's primary mirror would vary from 65 to 265 K at a 40 deg latitude, 0 deg longitude landing site.[5]

Structural trade studies compared the qualitative performance of various design schemes for the optical structures under thermal loading. It is anticipated that these results will be pertinent to the design of lunar-based telescopes in general, even if their thermal control systems are not passive. Trades resulted in the selection of a baseplate athermalized with respect to the mirrors, statically determinate mirror supports with three bottom-mounted flexures, and silicon carbide as the baseline mirror material.

Primary-Mirror Finite-Element Model

To conduct design trades for the LUTE optics, a finite-element model (FEM) of the primary mirror was built. Models were not built for the secondary and tertiary mirrors. Design decisions based on the response of the primary mirror were assumed to be applicable to the other mirrors.

The LUTE primary mirror, pictured in Fig. 2, has an outside diameter of 100 cm and an inside diameter of 50 cm. The internal mirror construction, pictured in Fig. 3, consists of two faceplates, 3 mm thick, separated by a 6-cm-thick sandwich core. The mirror also has a 2-mm-thick hatband around the outer circumference. Construction has not been optimized.

Received Sept. 8, 1993; presented as Paper 93-4776 at the AIAA Space Programs and Technologies Conference, Huntsville, AL, Sept. 21–23, 1993; revision received March 15,1994; accepted for publication March 17, 1994.

*Aerospace Engineer. Member AIAA.

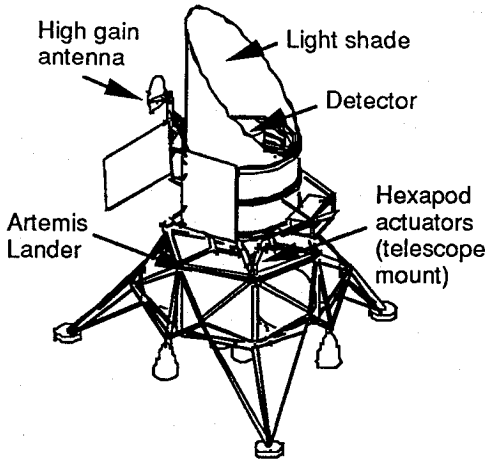

Fig. 1 LUTE telescope on Artemis lander.

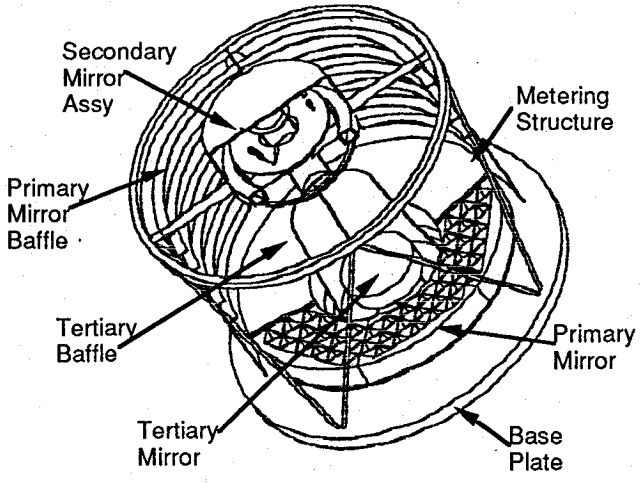

Fig. 2 LUTE optical bench.

The FEM has 192 nodes. The mesh increments are 6 cm vertically, 15 deg circumferentially, and 8.33 cm radially. There are 240 elements in the model. The faceplates are thin-shell linear quadrilateral elements, and the mirror's sandwich core is modeled with solid linear bricks. To approximate the sandwich construction, the solid elements were assigned a density equal to 5.3% of the material's normal value to simulate the sandwich cell mass and a Young's modulus equal to 3.5% of the material's normal value to simulate the honeycomb's stiffness.[6]

Mirror Material Candidates

Selection of the mirror material must be one of the first steps in the design of a telescope's optical structures. After the mirror material is selected, the baseplate material can be chosen. The choice of mirror material will also affect the selection of the mirror support and metering structure materials. The combination of mirror material and metering structure materials is critical in determinig the total system performance. A strain-free and thermally insensitive mirror is no good if the metering structure is sensitive to thermal loads. But if the mirrors and metering structure are the same material, or are otherwise athermalized, then temperature soaks can be compensated.

Material selection trades for the metering structure are beyond the scope of this paper. This paper focuses on material selection of the optics and baseplate, component by component. Room-temperature properties for the LUTE optical system material candidates are listed in Table 1.

There are many factors to be considered when selecting a suitable mirror material. An effort was undertaken to identify all comparison factors, or figures of merit, pertinent to a telescope's mirror material selection. Table 2 lists some of these comparison factors.

Mirror material trades and mirror support trades were complicated by the requirement that the optics withstand a lunar bulk temperature

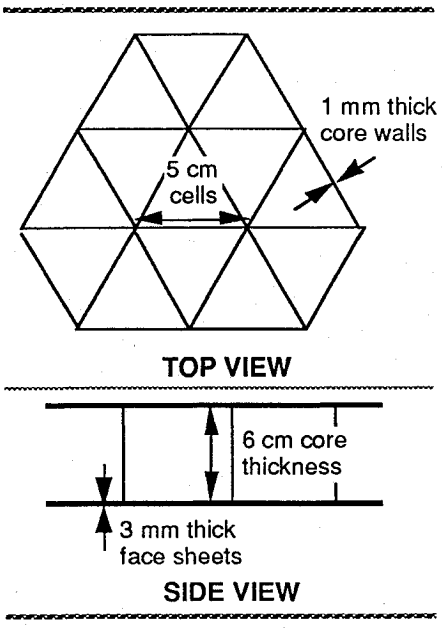

Fig. 3 Primary-mirror internal construction.

excursion of approximately 65 to 265 K. Ground- and space-based telescopes typically do not have to contend with the harsh thermal environment affecting lunar-based telescopes.[7] Consequently, the structural results presented herein focus primarily on the ability of a material to resist thermal loads. SSTDCs, TTDCs, and finite-element analyses of the primary mirror's surface figure in response to thermal loads will be discussed.

The TTDC, defined in Table 2, is a figure of merit that indicates a material's tendency to deform under transient thermal loads. Values of the TTDC near zero are considered good because they indicate that the material tends not to deform under transient thermal gradients at a given temperature. A plot of TTDC vs temperature is shown in Fig. 4.

Figure 4 was reproduced with permission from data presented by Paquin.[8] According to the plot, beryllium and Zerodur appear to resist transient thermal distortion better than other materials in the temperature range of 65 to 265 K.

However, the information displayed in Fig. 4 does not include some materials such as silicon carbide. Temperature-varying material properties of beryllium,[9,10] and silicon carbide[11] were obtained from literature and discussions with vendors. The TTDCs of these materials were then calculated and are plotted in Fig. 5. Figure 5 indicates that SiC tends to resist transient thermal deformations better than Be.

The SSTDC, defined in Table 2, is another figure of merit for a material's resistance to thermal deformation. Values of SSTDC near zero are considered good because they indicate that the material tends not to deform under steady-state thermal gradients at a given temperature. After temperature-varying material properties were obtained, the SSTDC was calculated and is plotted for Be, CVD SiC™, and CERAFORM® SiC[12] in Fig. 6. This figure indicates that SiC tends to resist steady-state thermal deformations better than Be.

The TTDC and SSTDC figures of merit provide some direction for the selection of a mirror material. Finite-element structural analyses will be used to compare the surface-figure thermal deformations of beryllium, silicon carbide, and fused silica primary mirrors.

Thermal Deformation Analyses

Thermal deformation analyses were utilized to characterize temperature effects, to study the interaction of the baseplate and optics material selection with respect to thermal deformations, to compare various concepts for the mirror support structure, and to conduct mirror material trades. Both hand and finite-element analyses were conducted.

Table 1 Room-temperature properties of candidate mirror materials

Material	Type	Density ρ, kg/m^3	YTS, MPa	Elastic modulus E, GPa	CTE, ppm/K	Conductivity k, W/m-K	Specific heat C_p, J/kg-K	Poisson's ratio μ
Beryllium[a,b]	O-50	1850	172	315	11.3	220	1875	0.042
Silicon dioxide	(quartz)[c]	2650	—	—	—	6.2–10.4	745	—
Silicon dioxide	(fused silica)[d]	2187	—	72	0.56	1.3	754[c]	—
Silicon[c]		2330	—	—	2.5[e]	148	712	—
Silicon Carbide	CVD[f]	3210	—	$\approx$ 463.5	1.9	193	$\approx$ 700	—
Silicon Carbide	CERAFORM[g]	2920	—	311	2.6	156	670	—
SiC/Al[h]	MMC	2910	—	117	12.4	123	1004	—
ULE[e,i]	Ti Silicate, 7971	2187–2205	UTS 50	68	0.054	1.3	766	0.17
Zerodur[e,j]	M	2519–2570	—	89	0.09	1.6	812	0.25

[a]Ref. 9.
[b]Ref. 10.
[c]Incropera and DeWitt, *Fundamentals of Heat and Mass Transfer*, 3rd ed., 1990, Appendix A, Table A.2.
[d]Dibble, M. A. (ed.) "Material Selection," *Machine Design: 1992 Basics of Design Engineering Reference Volume*, Vol. 64, No. 12, June 1992, p. 969.
[e]Ref. 13.
[f]Ref. 11.
[g]Ref. 12.
[h]Parsonage, T. "Selecting Mirror Materials for High-Performance Optical Systems," *Dimensional Stability*, SPIE Vol.1335, 1990, pp. 119–126.
[i]Anon., "ULE Titanium Silicate, Code 7971," Corning Glass Works, Corning, NY, (607) 974-4418, date unknown.
[j] Anon., "Glass Ceramics Zerodur M," Schott Glass Technologies Inc., Duryea, PA, (717) 457-7485, date unknown.

Table 2 Comparison factors for mirror material trades

Parameter	Definition	Units	Criteria
Specific stiffness	E/ρ	MJ/kg	High is good
Specific strength	YTS/ρ	kJ/kg	High is good
Microyield strength	stress producing 1% creep in 100,000 h.	MPa	High is good
Fracture toughness	K1c		
Anisotropy (property homogeneity)	Ratio of directional mat'l properties	Dimensionless	Near 1 is good
Hysteresis due to thermal cycling	Optical figure change	Waves rms	Low is good
Steady-state thermal distortion	CTE/k	cm/MW	Near 0 is good
Transient thermal distortion	CTE $\rho C_p/k$	μs/cm^2-K	Near 0 is good
Surface figure:	Departure to actual		
Peak-to-valley deformation	from undeformed	μm	Low is good
Curvature tilt		μ rad	Near 0 is good
Surface microroughness	Departure of surface from plane, rms	Å	Low is good
Optical scattering	Scattering from reflecting surface, rms	Å	Low is good
Bidirectional reflectance distribution function (BRDF)	(Reflected radiance)/ (incident irradiance)	sr^{-1}	Low is good
UV reflectance (normal incidence)	$R = [(n\lambda - 1)^2 + \lambda k^2]/[(n\lambda + 1)^2 + \lambda k^2]$	%	High is good
Cost	Price/diameter	$/cm	Low is good

Temperature Effects on Structures

A general feel and understanding for the temperature effects on structures will provide some valuable insights to guide the design of lunar-based telescopes. To illustrate, the characteristic deformations of a beam under three basic thermal load conditions are sketched in Fig. 7.

Hand analysis shows that a pure axial (through the thickness) temperature gradient is more significant than a pure diametral (across the span) temperature gradient in causing vertical deformation. For instance, in a beam with no constraints, having a span L and a thickness t, a diametral gradient of $(L/t)^2/2$ is needed to equal the vertical tip deflection caused by a 1-deg axial gradient. If the beam had a span of 50 cm and a thickness of 6.6 cm, a 28.7-deg diametral gradient would cause the same vertical tip deflection as a 1-deg axial gradient.

Athermalization

Athermalization means designing a structure so that its net deformation is insensitive to bulk temperature changes. Krim[13] discusses the concept of athermalization in detail. If care is not taken to athermalize lunar-based telescopes, bulk temperature excursions will drive the deformations. To illustrate, finite-element analyses were conducted with I-DEAS to evaluate the interaction between mirror thermal deformation and baseplate athermalization. A beryllium LUTE primary mirror was mounted to a baseplate via three flexures on the mirror's outside edge. The CTE of the baseplate was allowed to vary between 0 and 11.3 ppm/K (11.3 ppm/K equals the CTE of beryllium). The variation in baseplate CTE represented different candidates for the baseplate material selection. The thermal deformations of the primary mirror's figure, in response to an *assumed* temperature loading of 96-K bulk temperature excursion, 0.1-K axial gradient, and 0.6-K diametral gradient, are plotted in Fig. 8.

When the CTEs of the baseplate and optics match, at 11.3 ppm/K, the mirror's surface figure deformation is due solely to the axial and diametral temperature gradients. When the difference between the CTEs of the baseplate and optics becomes wider, however, the mismatch in their thermal growth results in larger deformations, due to the bulk temperature excursion.

Utilizing an athermalization scheme is strongly recommended for the baseplate-optics system and for any other sensitive component

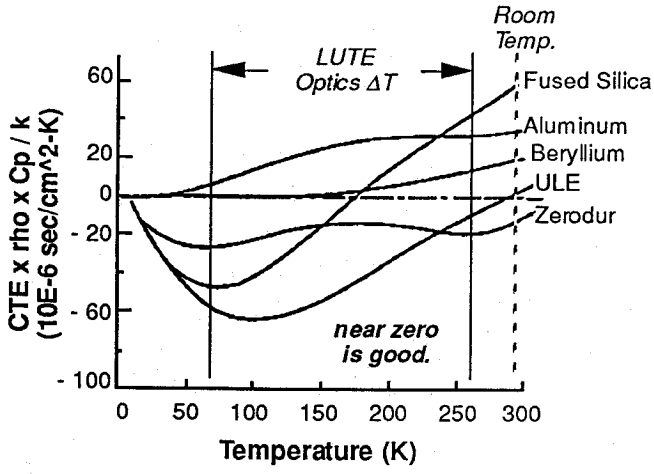

Fig. 4 Transient thermal distortion coefficient.[8]

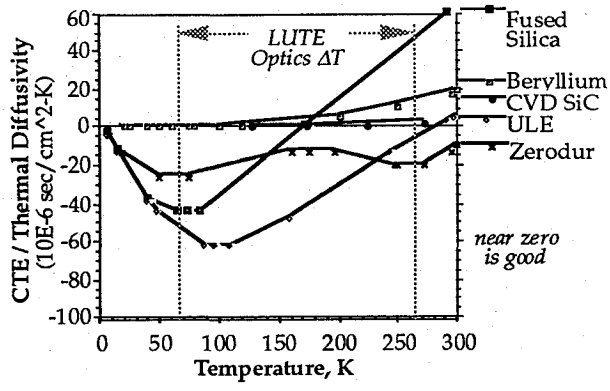

Fig. 5 Transient thermal distortion coefficient (plotted with beryllium and silicon carbide data).

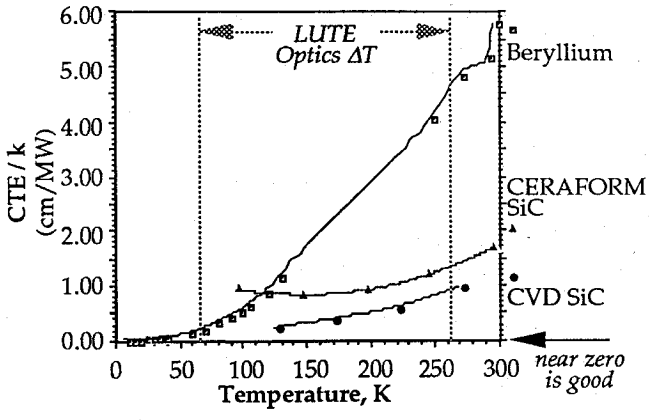

Fig. 6 Steady-state thermal distortion coefficient.

such as the metering structure. For the LUTE, athermalization plans are to match the CTEs of the baseplate and optics as closely as possible. Matching other thermal distortion indicators, such as the steady-state and transient thermal distortion coefficients, may also be necessary. The mirror support trade and mirror material trade, discussed later, assume an athermalized baseplate-optics system.

A concern, however, is whether athermalization can accommodate large bulk temperature swings (e.g., the 200-K range predicted for the LUTE optics). Athermalization schemes work best when the operating temperature is held within a narrow band, since the athermalized design can be tailored for those specific temperatures. If the temperature variation is outside this band, though, athermalization may break down. For example, given a metering strut design that has been athermalized using two different material configurations,

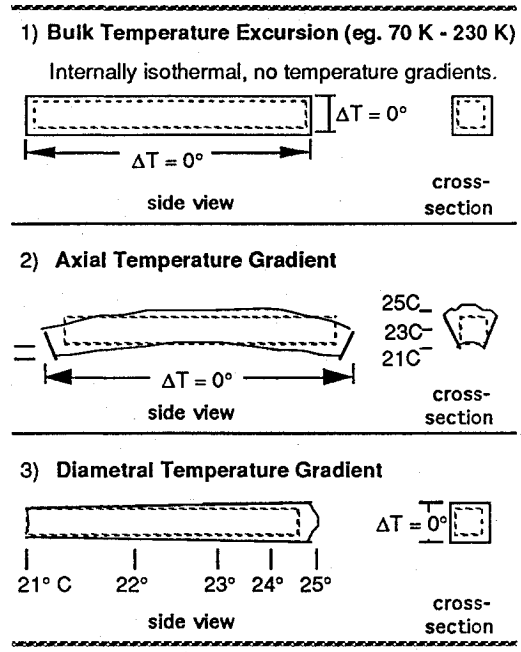

Fig. 7 Temperature effects on a beam

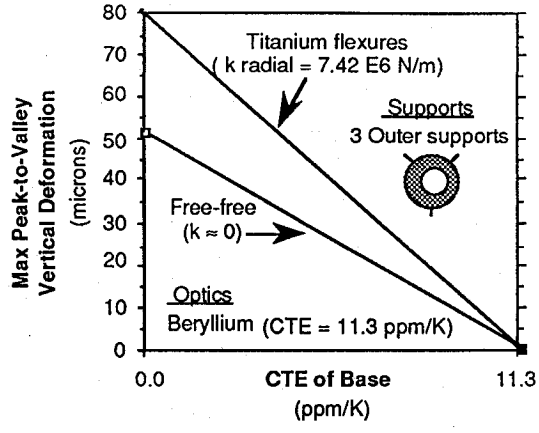

Fig. 8 Thermal deformation vs baseplate CTE.

there exists a ratio between the CTE's of the two materials[14] that allows the structure to be athermalized at a given temperature T_0:

$$\mathrm{AR} = \frac{\mathrm{CTE}_1(T = T_0)}{\mathrm{CTE}_2(T = T_0)} \tag{1}$$

If the temperature changes by an appreciable amount, the design will only remain athermalized if the ratio between thermal expansion slopes of the two materials also equals the AR:

$$\frac{\int(\partial \mathrm{CTE}_1/\partial T)\,dT}{\int(\partial \mathrm{CTE}_2/\partial T)\,dT} \approx \frac{(\partial \mathrm{CTE}_1/\partial T)\,\Delta T}{(\partial \mathrm{CTE}_2/\partial T)\,\Delta T} = \frac{(\partial \mathrm{CTE}_1/\partial T)}{(\partial \mathrm{CTE}_2/\partial T)} = \mathrm{AR} \tag{2}$$

Mirror Support Trade

Before a mirror material trade may be conducted, a design for the mirror support structure must be baselined. Structural supports for the primary and tertiary mirrors hold these optics above the baseplate and must allow the mirrors to expand and contract in the thermal environment. Otherwise, stress and additional warpage will be introduced into the mirrors. The mirror support trade was conducted to assess the effect of different mirror support concepts on a primary mirror's thermal deformations. The effect of mirror support stiffness on thermal deformations was also evaluated. Launch and lunar gravity loads were not considered in this trade.

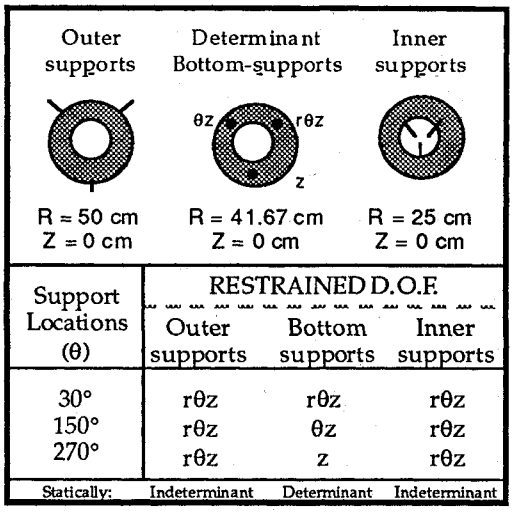

Fig. 9 Mirror support concepts.

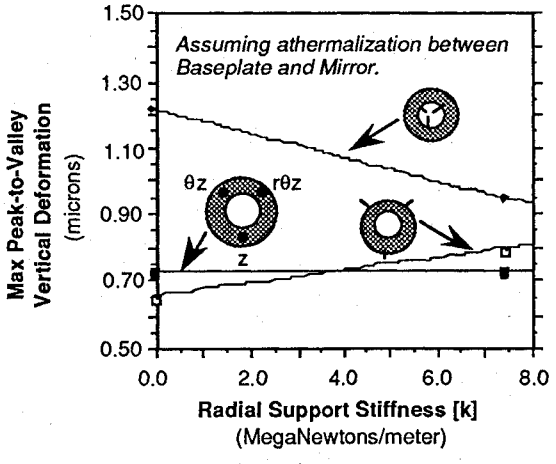

Fig. 10 Thermal deformation vs support concept.

Method

For the mirror support trade, the I-DEAS primary mirror FEM was assumed to be constructed with beryllium. An *assumed* temperature loading of 96-K bulk temperature excursion, 0.1-K axial gradient, and 0.6-K diametral gradient was applied to the model. The bottom surface of the mirror was supported along its outside edge, inside edge, and bottom with three flexures. The designs are illustrated in Fig. 9.

The bottom supports were radially mounted near the neutral surface of the mirror. The location of the neutral surface was estimated by calculating the radial balance point r, where the mirror's outer radial mass equaled the mirror's inner radial mass:

$$\pi\left(R_{\text{outer}}^2 - r^2\right)t\rho = \pi\left(r^2 - R_{\text{inner}}^2\right)t\rho = m_{\text{mirror}}/2 \qquad (3)$$

Equation (3) was then simplified to derive an equation for the radial balance point r:

$$r = \left(\frac{R_{\text{outer}}^2 + R_{\text{inner}}^2}{2}\right)^{\frac{1}{2}} \qquad (4)$$

Using Eq. (4), hand calculations approximated the primary mirror's neutral surface at a radial location of 39.5 cm. The bottom support in Fig. 9 are shown at 41.67 cm because this was the closest FEM nodal location to 39.5 cm.

The outer, inner, and bottom supports were modeled with spring elements. Several runs were made with each design to assess the thermal deformations as the spring constants were varied. These deformations are plotted in Fig. 10.

Table 3 Thermal-structural performance of three primary mirror materials

	Thermal load		Surface figure	
Time	Average temperature, K	Temperature gradient, K	Peak-to-valley deformation,[a] μm	Curvature tilt,[b] μdeg
	a) *Silicon carbide (CERAFORM®)*[c]			
Noon	261.3	0.20	*0.048*	*10.66*
Afternoon	157.1	0.09		
	b) *Beryllium O-50*[d]			
Morning	123.2	0.11	0.035	13.42
Noon	261.2	0.18	*0.160*	*55.75*
Afternoon	159.5	0.09	0.054	−15.70
	c) *Fused silica*[e]			
Morning	177.7	7.07	0.459	794.66
Noon	260.1	3.34	0.210	197.53
Afternoon	159.0	7.80	*0.460*	*−873.50*

[a]Low is good.
[b]Near zero is good.
[c]Room-temperature material properties, except CTE at $f(T)$. Assumed Poisson's ratio = 0.25. Best material.
[d]Temperature-varying properties.
[e]Room-temperature material properties. Worst material.

Results

Figure 10 indicates that the resulting deformations for the inner supports were worse than for the outer supports and bottom supports. The results were not conclusive in showing whether bottom support deformations are better than outer support deformations. The assumed thermal loads were not large enough to create a significant difference between these options.

The bottom support, however, has the advantage of not being influenced by the stiffness of the flexures because it is statically determinate. Therefore, the statically determinate support concept with three bottom-mounted flexures was chosen as the baseline design for the LUTE mirrors. Future mirror support trades, unlike the trade just described, should analyze the outer, inner, and bottom supports when they are *all* either statically determinate or statically indeterminate, to insure consistency in the trade. Future trades should also use larger thermal loads, so that the trade results will be more discernible.

Mirror Material Trade: Figure Deformations Under Thermal Loads

After the athermalized baseplate-optics design and the statically determinant support concept with bottom-mounted flexures were baselined for the LUTE preliminary design, a mirror material trade was conducted. The trade used finite-element analyses to calculate thermally induced figure deformations of the primary mirror during lunar operation. The thermal load applied to the finite-element models represented an isothermal lightshade and baseplate at a 40 deg latitude, 0 deg longitude landing site.[15] Beryllium, silicon carbide, and fused silica were compared during the study.

Beryllium Thermal Deformations

The detailed thermal deformation results for a beryllium primary mirror will be presented. Beryllium was the first material analyzed, owing to the ready availability of its temperature-varying material properties and its low mass. Silicon carbide and fused silica were then analyzed. Only the summarized results for silicon carbide and fused silica will be presented.

Figure 11 illustrates the maximum thermal deformations calculated with I-DEAS/Model Solution for the beryllium LUTE primary mirror. This represents only one thermal-load case, the temperature case causing maximum thermal deformation. In all, beryllium primary-mirror temperatures and deformations were calculated for three critical time steps during the lunar day night thermal cycle. The output temperatures and deformations are summarized in Table 3b.

The time steps in Table 3b were chosen because the largest temperature gradients in the mirror existed at those times. The bulk temperature range was 65 to 262 K. The maximum vertical peak-to-valley thermal deformation was about 0.16 μm, with a maximum

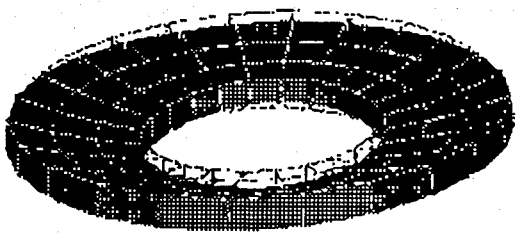

a) Thermal distortion

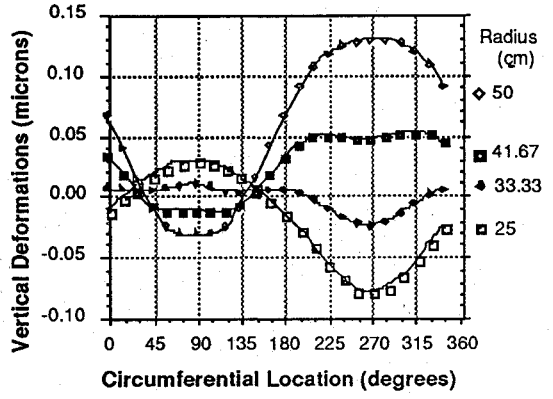

b) Vertical deformations around circumference

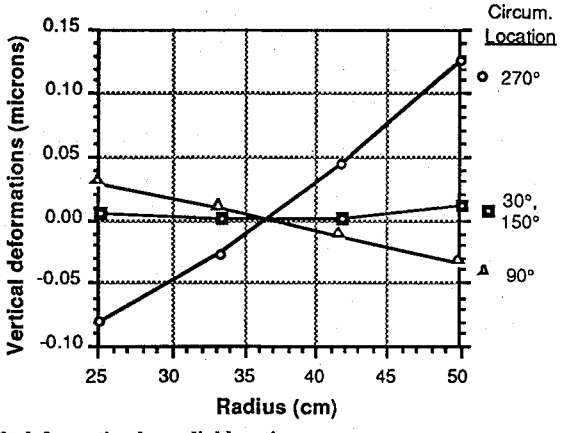

c) Tilt deformation by radial location

Fig. 11 Beryllium primary-mirror thermal-deformations.

curvature tilt of about 56 μdeg. The maximum thermal stress in the mirror was 102.6 kPa, resulting in a high margin of safety.

Thermal-Deformation Trade Results

Similar FEM analyses were conducted with I-DEAS/Model Solution for a silicon carbide and fused silica primary mirrors. Thermal-deformation results for beryllium, silicon carbide, and fused silica are summarized in Table 3. The thermal stresses developed in all three materials were low, below 1 MPa, and acceptable.

Table 3 shows that SiC resisted thermal deformation better than the other two mirror materials, since its maximum surface-figure deformations were the lowest. The qualitative results from this material trade, based on FEM analysis of the thermal deformations, concurred with the T TDC and SSTDC material property comparisons in Figs. 5 and 6. As a result, silicon carbide was chosen as the baseline mirror material for the LUTE preliminary design.

Note that the SiC structural analysis was based on room-temperature properties, except for the CTE, which was taken as a function of temperature. Typical temperature-varying properties for SiC from 65 to 265 K will be better than the room-temperature properties. Therefore, the tabulated thermal deformations for SiC represent worst-case scenarios. The qualitative ranking in Table 3 will still hold if temperature-varying properties are used for SiC in a more detailed analysis.

Conclusion

Degradation of the optical performance due to thermal deformations during the lunar day night cycle was the driving concern of the LUTE preliminary design study. This task necessitated close interaction between the materials, configuration, thermal, structures, and optics disciplines.

Three modes of thermal loading—bulk temperature excursion, axial temperature gradient, and diametral temperature gradient—on the optics were identified. Axial gradients are more significant than diametral gradients in causing thermal deformations. However, structural analyses indicated that the primary-mirror bulk temperature excursion during the lunar day night cycle will drive the figure deformations in the optics unless the primary mirror and baseplate are athermalized with respect to each other. Athermalization, in this case, may be accomplished by matching thermal-distortion similarity parameters for the optics and baseplate, such as the coefficients of thermal expansion and the transient thermal distortion coefficients. A concern, however, is whether athermalization can accommodate the large bulk temperature swings predicted for the LUTE.

Two trade studies for the primary mirror were discussed: a mirror support trade and a mirror material trade. The mirror support trade evaluated various inner, outer, and bottom support concepts. Analyses based on an assumed thermal loading of a beryllium primary mirror, indicated that inner supports were worse than the other concepts, since the thermal deformations were larger. Outer supports and bottom supports resulted in similar deformations. However, kinematic bottom supports had the advantage of being statically determinate. As a result, a statically determinate support with three bottom-mounted flexures was baselined. Using this support configuration, a finite-element mirror material trade evaluated the thermal deformations of a beryllium, a silicon carbide, and a fused silica primary mirror. At the selected 40 deg longitude, 0 deg latitude landing site, the maximum peak-to-valley and curvature-tilt primary-mirror deformations were smaller with silicon carbide than with beryllium or fused silica. Silicon carbide has therefore been baselined as the mirror material for the LUTE preliminary design.

Acknowledgments

The author wishes to express his appreciation to Mark Gerry of the NASA Marshall Space Flight Center (MSFC) for providing the configuration drawings of the LUTE telescope and optical bench, to Sherry Walker and Reggie Alexander of MSFC for performing the thermal analysis of the optics, and to Bill Jones of MSFC for many insightful discussions on optics and for performing the optical analysis.

References

[1]McBrayer, Frazier, and Nein, "Lunar Ultraviolet Telescope Experiment (LUTE) Overview," AIAA Paper 93-4740, Sept. 1993.

[2]McGraw, J. T., "LUTE: A UV Strip Search of the Universe," AIAA Paper 93-4772, Sept. 1993.

[3]Cremers, Birkebak, and White, "Thermal Characteristics of the Lunar Surface Layer," *International Journal of Heat and Mass Transfer*, Vol. 15, May 1972, pp. 1045–1055.

[4]Walker, S., and Alexander, R., "LUTE Thermal Control System Analysis and Design," PD22-92-15, NASA/George C. Marshall Space Flight Center, Huntsville, AL, Dec. 1992, Sec. 2.8.3.

[5]McCarter, J. W., "Site Selection and its Influence on the Design of a Lunar-Based Telescope," AIAA Paper 93-4774, Sept. 1993, p. 10.

[6]Anon, "Mechanical Properties of Hexcel Honeycomb Materials," TSB 120, Hexcel Corp., Structural Div. Dublin, CA, 1992.

[7]Walker, S. T., and Alexander, R. A., "The Impact of the Lunar Thermal Environment on the Design of Telescopes for Lunar Surface Operation," AIAA Paper 93-4775, Sept. 1993. p. 2.

[8]Paquin, R., "Hot Isostatic Pressed Beryllium for Large Optics," *Optical Engineering*, Vol. 25, No. 9, 1986, p. 1004.

[9]Killpatrick, D. H., "Report on the Properties of Beryllium," RDA Logicon, Albuquerque, NM, prepared for Oak Ridge National Laboratory, Oak Ridge, TN, May 1990, pp. 12–14, 24–28, 76–77, 95, 96, 153–155.

[10]Swenson, "HIP Beryllium: Thermal Expansivity form 4 to 300 K and Heat Capacity from 1 to 108 K," *Journal of Applied Physics*, Vol. 70, No. 6, Sept. 1991.

[11]Anon., "CVD Silicon Carbide™," CVD Materials Technical Bulletin 107, Morton Advanced Materials, Woburn, MA, 1990.

[12]Anon., "UTOS CERAFORM® Silicon Carbide (Siliconized SiC)," United Technologies Optical Systems, West Palm Beach, FL, date unknown.

[13]Krim, M., "Selected Topics on the Athermalization of Optical Structures," SPIE Short Course, Hughes Danbury Optical Systems, Danbury, CT, 1992.

[14]Krim, M. H., "Design of Highly Stable Optical Support Structure," *Optical Engineering*, Vol. 14, No. 6, 1975, p. 557.

[15]Walker, S., and Alexander, R., "LUTE Thermal Control System Analysis and Design," NASA/George C. Marshall Space Flight Center, PD22-92-15, Huntsville, AL, Dec. 1992, Sec. 2.8.3.